ELSEVIER

Journal of Power Sources 89 (2000) 232–236

JOURNAL OF POWER SOURCES

www.elsevier.com/locate/jpowsour

Structural aspects of electrochemically lithiated SnO: nuclear magnetic resonance and X-ray absorption studies

Y. Wang [a], J. Sakamoto [b,1], S. Kostov [a], A.N. Mansour [c], M.L. denBoer [a,*], S.G. Greenbaum [a], C.-K. Huang [b], S. Surampudi [b]

[a] *Physics Department, Hunter College of City University of New York, New York, NY 10021, USA*
[b] *Electrochemical Technologies Group, Jet Propulsion Laboratory, California Institute of Technology, Pasadena, CA 91109, USA*
[c] *Naval Surface Warfare Center, 9500 MacArthur Boulevard, West Bethesda, MD 20817, USA*

Received 24 September 1999; accepted 14 October 1999

Abstract

We have compared the local structure of electrochemically lithiated SnO with Sn/Li alloys using ^{7}Li to study the environment of the Li ion and extended X-ray absorption fine structure to study the environment of the Sn ion. Although a widely accepted simple model suggested that the electrochemically lithiated SnO should be similar to Sn/Li alloys of corresponding composition, we find this is true only at low Li concentrations. The addition of more Li to the structure produces, for both the Li and the Sn, features which are difficult to reconcile with the simple model, and suggest the presence of direct Sn–O interactions.

Keywords: SnO; Nuclear magnetic resonance; X-ray absorption

1. Introduction

Tin compounds and especially oxides have attracted recent interest as high capacity anodes in lithium ion batteries [1–7]. The compound SnO, which has been considered as a possible anode material, has the additional advantage of serving as a useful model of the more chemically complex composite tin oxide glasses. A widely used model of the reaction of lithium with SnO involves initially reduction of the Sn and subsequently alloying of the Sn, according to [1,2]:

$$SnO + xLi \rightarrow Li_2O + SnLi_{x-2}. \quad (1)$$

Although there is a large irreversible Li capacity associated with the Li_2O phase, the latter appears to improve cyclability as compared to elemental Sn, which undergoes large volumetric changes on Li alloying. Recently published results from our laboratory [4] and others [5–7] have shed additional light on the electrochemical lithiation of SnO, via ^{7}Li nuclear magnetic resonance (NMR) and X-ray absorption spectroscopy at the Sn K-edge. The two methods are complementary in that the former yields information regarding the local environment of the Li^{+} ions while the latter is sensitive to the local Sn environment. In these previous studies, it was found that the simple reaction mechanism (1) is valid only under limited circumstances; large structural differences between the ideal SnLi alloy and the electrochemically lithiated material were observed at high Li content [4–7]. In this paper, we present more detailed measurements than those in our initial communication [4], which provide additional evidence for differences in alloy formation at high Li content.

2. Experimental

Lithium was electrochemically titrated into SnO as described elsewhere [4] under galvanostatic (20 $\mu A/cm^2$) conditions. Reference $SnLi_x$ alloys were synthesized by direct reaction of the elements. Appropriate amounts of elemental lithium and tin obtained commercially were weighed. Tin contained in a molybdenum crucible was

* Corresponding author. Tel.: +1-212-772-5258.
E-mail address: mdenboer@hunter.cuny.edu (M.L. denBoer).
[1] Current address: Department of Materials Science, University of California at Los Angeles, Los Angeles, CA 90095, USA.

0378-7753/00/$ - see front matter
PII: S0378-7753(00)00434-1

first melted in an oven within a glove box under argon. Lithium was then added to the molten Sn. The final products were annealed at 350°C for 24 h and the resulting alloys were ground into powder.

Solid state ^{7}Li NMR measurements were performed with a Chemagnetics CMX 300 spectrometer operating at a resonance frequency of 117 MHz. Both wide line and high resolution magic angle spinning (MAS) spectra were acquired, the latter with a spinning rate of about 5 kHz. A 1-M aqueous solution of LiCl was employed as a chemical shift reference.

Samples were prepared for EXAFS measurements by mixing $SnLi_x$ and $SnOLi_x$ alloys with boron nitride and pressing the material into pellets, measured to be one absorption length thick at the Sn K edge, under argon atmosphere in a dry glove box. The XAS experiments were performed on experimental station X-11A of the National Synchrotron Light Source with the electron storage ring operating at an electron energy of 2.8 GeV and stored current in the range of 110 to 250 mA. Data were collected with a variable exit double-crystal monochromator using two flat Si (311) crystals. The energy resolution at the Sn K-edge energy, taking into account the incident beam slit width of 0.5 mm at a distance of 10 m from the source, is 10.2 eV. At the Sn K-edge energy, the harmonics content of the beam is negligible and the monochromator was not detuned. The incident and transmitted X-ray intensities were monitored using ionization chambers (30 cm in length) filled with argon gas. The XAS measurements were made in transmission mode at room temperature. A Sn foil reference was used for calibration.

The Sn K edge EXAFS spectra provide information about the local Sn environment. Analysis involves subtraction of the background from the raw absorption spectra, conversion to k-space and Fourier transformation to r-space, yielding a quasi-radial distribution function (QRDF) centered at the absorbing Sn ion. Peaks in this function correspond to near neighbor distances. Changes in the local Sn environment which occur with lithiation can be quantitatively compared to model functions theoretically calculated using the program FEFF [8].

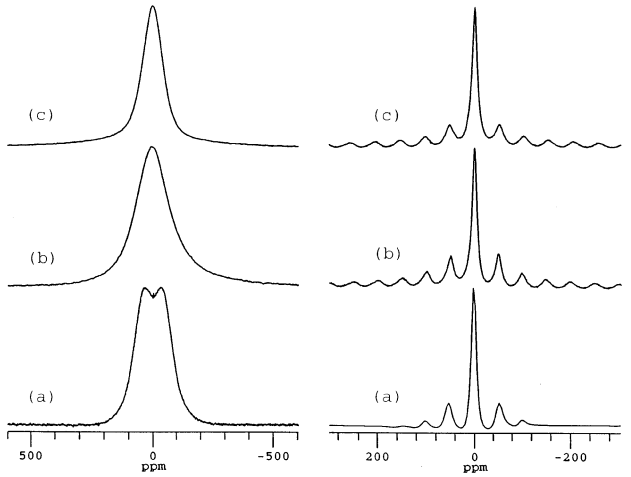

Fig. 2. NMR spectra of ^{7}Li; wide line (left side) and MAS (right side) in (a) crystalline Li_2O; (b) $SnO/Li_{0.5}$; and (c) $SnO/Li_{2.0}$.

3. Results and discussion

A typical electrochemical titration curve of Li in SnO for the materials in this investigation, presented in a previous publication [9], is shown in Fig. 1. Full lithiation (0 V vs. Li) corresponds to a stoichiometry of 6.4 Li per SnO. This is in agreement with the simple model (Eq. 1) assuming that the maximum Li content of the pure alloy is $SnLi_{4.4}$, as implied by the known phase diagram of SnLi

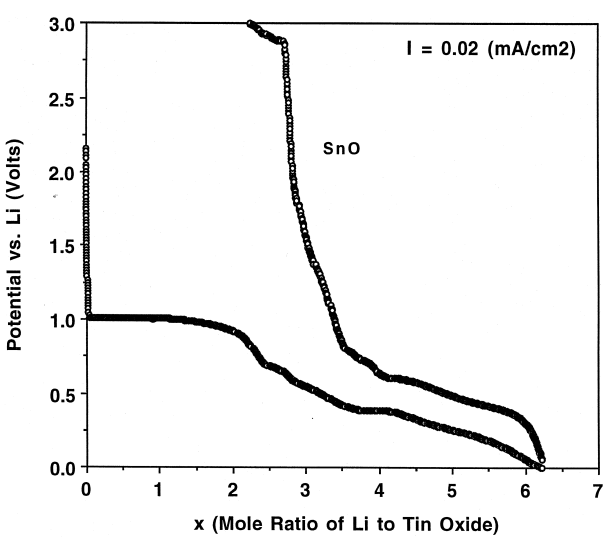

Fig. 1. Electrochemical titration curve for Li in SnO.

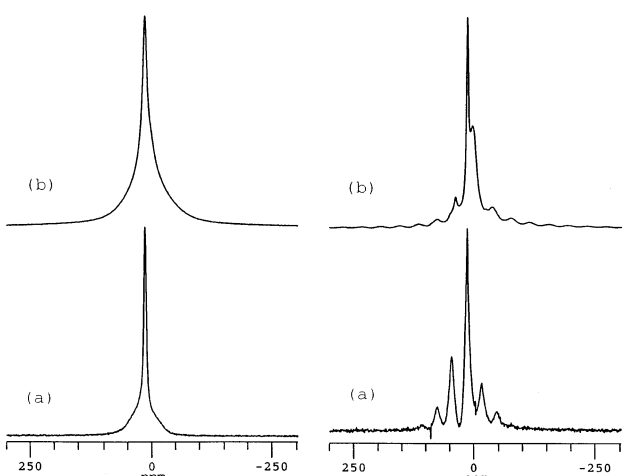

Fig. 3. NMR spectra of ^{7}Li; wide line (left side) and MAS (right side) in (a) $SnLi_{2.3}$ and (b) $SnO/Li_{4.3}$.

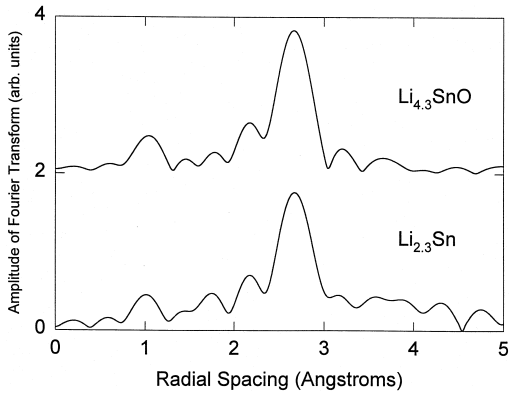

Fig. 4. EXAFS QRDF of $SnO/Li_{4.3}$ (upper curve) and $SnLi_{2.3}$ alloy (lower curve). These are very similar, as expected from the simple reaction model.

alloys [3]. On electrochemical delithiation, 2.0 Li per SnO remain in the material, again consistent with the formation of Li_2O as implied by Eq. (1). Previous X-ray diffraction studies [2] failed to detect the presence of crystalline Li_2O, leading to the conclusion that the Li_2O formed on electrochemical reduction of SnO is amorphous.

This conclusion is supported by the wide line and MAS ^7Li NMR spectra of samples SnO/Li_x, for $x = 0.5$ and 2.0, displayed in Fig. 2 with spectra of commercial (Aldrich) crystalline Li_2O as a reference. The model (Eq. 1) predicts that for $x < 2.0$ the only lithium-containing compound in the electrochemically titrated material is Li_2O. However, it is evident from Fig. 2 that the spectra of the former are considerably different from those of the latter. In the wide line spectra, the Pake doublet (due to the ^7Li–^7Li dipolar interaction) observed in the crystalline Li_2O is not resolved in the SnO/Li materials. In the MAS spectra, the latter also yield broader side band spinning

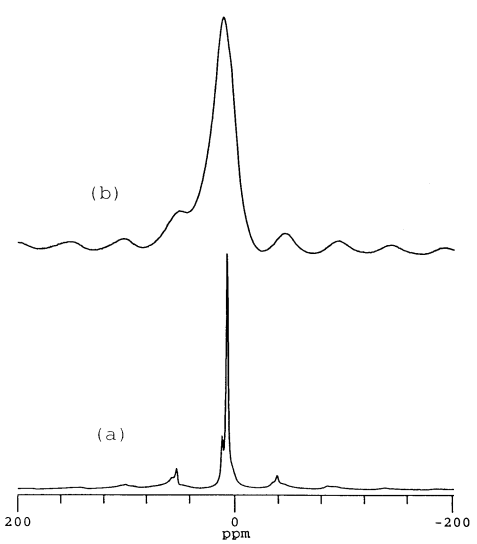

Fig. 5. Magic angle spinning NMR spectra of ^7Li in (a) $SnLi_{3.5}$ and (b) $SnO/Li_{5.5}$.

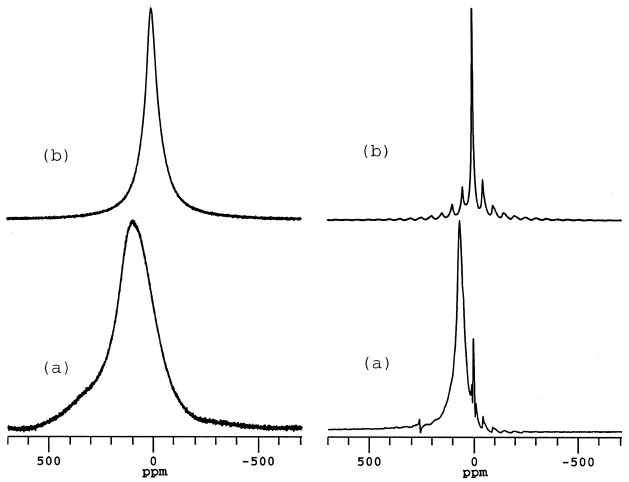

Fig. 6. NMR spectra of ^7Li; wide line (left side) and MAS (right side) in (a) $SnLi_{4.4}$ and (b) $SnO/Li_{6.4}$.

patterns than the Li_2O reference. Both of these observations imply that the Li_2O in the SnO/Li materials is amorphous. A distribution of Li–O–Li angles in a disordered analogue of the crystalline compound would smear out the Pake doublet characteristic of the latter and would also yield a broader side band pattern, because MAS is not as effective in narrowing spectral features due to distributions (i.e. inhomogeneous broadening). MAS is also less effective in averaging interactions appreciably broader than the spinning frequency. Parenthetically, note that the wide line spectrum of the $x = 0.5$ compound exhibits additional broadening, which we attribute to a larger relative contribution to the spectrum from lithiated electrolyte decomposition products, similar to the solid electrolyte interphase present in lithiated graphite [10].

At higher ($x > 2$) Li content, the simple model (Eq. 1) implies that the Li alloys with the Sn. This is confirmed by the wide line and MAS ^7Li NMR spectra of $SnO/Li_{4.3}$ and the corresponding reference alloy $SnLi_{2.3}$ shown in

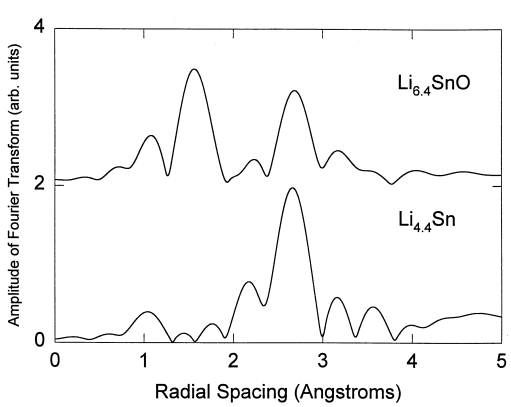

Fig. 7. EXAFS QRDF spectrum of $SnO/Li_{6.4}$ (upper curve) and $SnLi_{4.4}$ (lower curve). The drastic differences seen are inconsistent with the simple model.

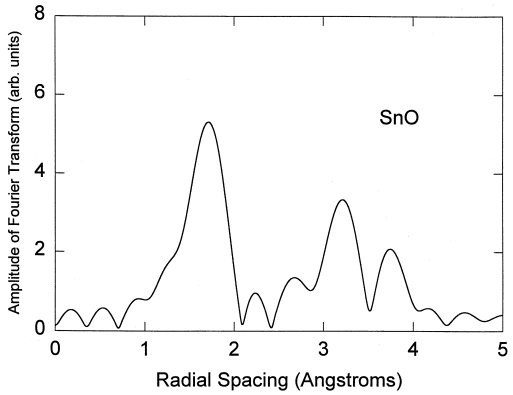

Fig. 8. EXAFS QRDF spectrum of SnO.

Fig. 3. Under both sets of experimental conditions, the $SnO/Li_{4.3}$ spectrum is well approximated by a superposition of the $SnLi_{2.3}$ alloy, with major components appearing at about 17 and 47 ppm, and amorphous Li_2O, consistent with the simple model and with the NMR results of Ref. [7].

This confirmation of the simple model is reinforced by EXAFS, which as mentioned, studies the local environment of the Sn. In Fig. 4, we compare the QRDFs of $SnLi_{2.3}$ and $SnO/Li_{4.3}$. The dominant peak corresponds to the nearest Sn–Sn distances, which are slightly decreased with respect to the distances measured for the beta phase of metallic Sn, in agreement with previous studies[5–7]. The close similarity between the peak structure of $SnLi_{2.3}$ and $SnO/Li_{4.3}$ is consistent with full reduction of the Sn in the latter and the formation of $SnLi_{2.3}$ alloy particles. There is no evidence of Sn–O interactions within the first coordination shell. Like the NMR results which study the Li sites, this is consistent with the simple reaction model.

However, both the NMR and EXAFS results imply the simple model does not work at higher Li content. The NMR MAS spectra of $SnO/Li_{5.5}$ and the reference alloy $SnLi_{3.5}$, shown in Fig. 5, differ by more than merely the addition of an amorphous Li_2O component to the latter. Although the major $SnLi_{3.5}$ alloy spectral components appearing at 8, 12, and 55 ppm are also present in the electrochemically prepared $SnO/Li_{5.5}$, the latter has a considerably broader line width, indicating a more heterogeneous Li environment. At the maximum Li content, the difference between the Li environments in the lithiated SnO and the corresponding reference alloy is even more dramatic. Both wide line and MAS spectra of $SnO/Li_{6.4}$ and $SnLi_{4.4}$ are shown in Fig. 6. While the reference alloy is characterized by a major Knight-shifted component at around 69 ppm and a small component at 260 ppm, the latter corresponding to metallic Li, the $SnO/Li_{6.4}$ sample exhibits only a single prominent peak at 8 ppm (apart from the amorphous Li_2O component at 0 ppm).

Similarly, Fig. 7 shows the EXAFS QRDF for the $Li_{4.4}Sn$ alloy and the electrochemically produced $SnO/Li_{6.4}$. These distribution functions do not resemble each other, indicating that the local Sn environment of the alloy is very different from that of the electrochemically produced material. There appears to be Sn–O bonding, as evidenced by the prominent peak around 2.1 Å (after phase shift correction; in Fig. 7 the peak appears at ~1.6 Å), a distance which is similar to the first Sn–O coordination shell found by others [7] at low Li concentration in both the charge and discharge part of the voltage cycle. This distance differs slightly, but significantly, from the measured first shell O distance (2.2 Å) in SnO (Fig. 8). The reappearance of O bonding at high Li content is very unexpected and requires further investigation. This surprising result may be related to possible oxygen uptake and reintroduction into the coordination shell, as suggested in Ref. [7], or a previously reported observation [11] that electrochemically prepared alloys differ from metal alloys formed under thermal equilibrium.

4. Conclusion

Both the NMR and EXAFS results confirm that at low Li concentration, the simple model of the electrochemical reaction, which assumes the formation of Li_2O followed by the alloying of Li with Sn, is correct. The local environment of the Li, as measured by ^{7}Li NMR, and the local environment of the Sn, as measured by EXAFS on the Sn K edge, are consistent with the presence of these species. On the other hand, as the electrochemical reaction continues and more Li is introduced into the structure, this simple model appears to break down and other species form. There are indications of direct Sn–O interactions at the highest Li concentrations.

Acknowledgements

This research was supported by the NASA Mars Exploration Program Office, the Department of Energy and the Office of Naval Research. One of the authors (SGG) acknowledges the National Research Council for fellowship support during his recent sabbatical leave at JPL.

References

[1] Y. Idota, T. Kubota, A. Matsufuji, Y. Maekawa, T. Miyasaka, Science 276 (1997) 1395.
[2] I.A. Courtney, J.K. Dahn, J. Electrochem. Soc. 144 (1997) 2045.
[3] R.A. Huggins, Solid State Ionics 113–115 (1998) 57.
[4] Y. Wang, J. Sakamoto, S.G. Greenbaum, C.K. Huang, S. Surampudi, Solid State Ionics 110 (1998) 167.
[5] A.N. Mansour, S. Mukerjee, X.Q. Yang, J. McBreen, J. Synchrotron Radiat. 6 (1999) 596.

[6] A.N. Mansour, S. Sanjeev, X.Q. Yang, J. McBreen, in: S. Surampudi, R.A. Marsh (Eds.), Lithium Batteries, The Electrochemical Society Proceedings Series, Pennington, NJ, 1999, p. 151, PV98-16.
[7] G.R. Goward, W.P Power, F. Leroux, G. Ouvard, W. Dmowski, T. Egami, L.F. Nazar, Electrochem. Solid-State Lett. 2 (1998) 367.
[8] J.J. Rehr, R.C. Albers, S.I. Zabinsky, Phys. Rev. Lett. 69 (1992) 3397, Ab initio Multiple-Scattering X-ray Absorption Fine Structure and X-ray Absorption Near Edge Structure Code, Copyright 1992, 1993, FEFF Project, Department of Physics, FM-15 University of Washington, Seattle, WA 98195.
[9] C.-K. Huang, J.S. Sakamoto, M.C. Smart, S. Surampudi, J. Wolfenstine, Mater. Res. Symp. Proc. 496 (1998) 519.
[10] Y. Dai, Y. Wang, S.G. Greenbaum, V. Eshkenazi, E. Peled, J. Electrochem. Soc. 145 (1998) 1179.
[11] J.R. Dahn, I.A. Courtney, O. Mao, Solid State Ionics 111 (1998) 289.